DOI: 10.1002/ejic.200700455

Two Novel Species, (Methoxycarbonyl)sulfenyl Thiocyanate and (Methoxycarbonyl)sulfenyl Selenocyanate: Spectroscopic Characterization by Photoelectron Spectroscopy and Quantum Chemical Investigation

Lin Du,[a,b] Li Yao,[a,b] and Maofa Ge*[a]

Keywords: Ab initio calculations / Dichalcogens / Electronic structure / Photoelectron spectroscopy

Two novel dichalcogens, (methoxycarbonyl)sulfenyl thiocyanate, $CH_3OC(O)SSCN$, and (methoxycarbonyl)sulfenyl selenocyanate, $CH_3OC(O)SSeCN$ have been generated in a convenient way by gas-solid reactions between $CH_3OC(O)SCl$ and AgSCN or AgSeCN. Photoelectron spectroscopy and theoretical calculations have been performed to investigate their electronic and geometrical structures. Both compounds are theoretically predicted to prefer *gauche* structure as the most stable conformation. In $CH_3OC(O)SSCN$, the S–S bond length and the dihedral angle around the S–S bond for the most stable conformer are 2.075 Å and 80.5°, respectively. And the S–Se bond length and the dihedral angle around the S–Se bond in $CH_3OC(O)SSeCN$ are predicted to be 2.210 Å and 80.4°, respectively. The first vertical ionization energies of $CH_3OC(O)SSCN$ and $CH_3OC(O)SSeCN$ are determined to be 10.19 and 9.84 eV, respectively. The HOMOs correspond to the electron mainly localized on the S 3p or Se 4p lone pair MOs: $\{38a(n_{S(SCN)})\}^{-1}$ and $\{47a(n_{Se})\}^{-1}$, respectively.

1. Introduction

In recent years, it has been found that chalcogen–chalcogen interactions play a crucial role in the structure and reactivity of a great variety of chalcogen-containing compounds.[1,2] The chalcogen–chalcogen bonds in bivalent compounds (REE′R′, E, E′ = O, S, Se) are known to prefer *gauche* conformations, which is usually attributed to lone-pair interactions.[3] These interactions favor a dihedral angle of about 90°, and steric interactions between the substituents (R, R′) tend to increase this angle. There are many experimental studies about the structural and conformational properties of homonuclear dichalcogens ROOR′,[4,5] RSSR′,[6,7] and RSeSeR′.[8,9]

In 1977, Snyder et al.[10] discussed the lone pair interactions in RSSR vs. RSOR by means of semiempirical MO calculations. Particular attention was paid to the α-lone pair interactions, and the study concluded that the two species were predicted to exhibit comparable equilibrium geometries. Because of the instability of thioperoxides RSOR′, until recently, only a few experimental studies were performed to investigate their structural and conformational properties.[11–13] Very recently, the parent compound of thioperoxides, HSOH was studied by microwave spectroscopy and high-level ab initio calculations [CCSD(T)/cc-pCVQZ],[14] which demonstrated its structure in detail. As for the experimental studies of the electronic structure of thioperoxides, dimethoxysulfane $[(CH_3O)_2S]$ and dimethoxydisulfane $[(CH_3O)_2S_2]$ were discussed according to their photoelectron spectra.[15] In 2006, Zeng et al.[16] investigated bis(trifluoroaceto) disulfide, $CF_3C(O)OSSOC(O)CF_3$, by Raman, photoelectron spectroscopy (PES), and theoretical calculations.

The electronegativity of selenium is close to that of sulfur. Therefore, similar structural and spectroscopic characteristics are expected in the selenium and sulfur derivatives.[17] As for the studies of sulfenoselenates with the general formula RSSeR′, there were some theoretical investigations about HSSeH,[18–20] and the crystal structure of NCSSeSCN[21] was also reported. In 2003, Sanz et al.[22] investigated the gas-phase acidity of 1,8-chalcogen-bridged naphthalenes, which also possess the S–Se bond, by means of high-level density functional theory computations.

However, there is no experimental work reported of RSSeR′, and no electronic structure information is currently available. They are quite unstable and difficult to obtain for experimental detection. In the present work, a simple dichalcogen hydride, (methoxycarbonyl)sulfenyl selenocyanate $[CH_3OC(O)SSeCN]$, was generated and characterized by photoelectron spectroscopy. With the help of quantum chemical calculations, its geometric structure was theoretically predicted and its electronic structure was discussed. The first vertical ionization energy of $CH_3OC(O)$-

[a] Beijing National Laboratory for Molecular Sciences (BNLMS), State Key Laboratory for Structural Chemistry of Unstable and Stable Species, Institute of Chemistry, Chinese Academy of Sciences,
100080 Beijing, P. R. China
Fax: +86-10-62559373
E-mail: gemaofa@iccas.ac.cn
[b] Graduate University of Chinese Academy of Sciences,
100039 Beijing, P. R. China
Supporting information for this article is available on the WWW under http://www.eurjic.org/ or from the author.

SSeCN was determined for the first time by means of PES. In addition, a novel disulfide, (methoxycarbonyl)sulfenyl thiocyanate [$CH_3OC(O)SSCN$], which has a similar structure to $CH_3OC(O)SSeCN$, was generated and characterized with the same method for comparison.

2. Results and Discussion

2.1 Molecular Structure

For both compounds, stable conformers with synperiplanar (sp) or antiperiplanar (ap) orientation of the C=O bond with respect to the S–S or S–Se bond are expected. Preliminary structure optimizations at the B3LYP/6-31G* level resulted in *gauche* structures around the S–S or S–Se bond. The potential functions for internal rotation around the S–S bond in $CH_3OC(O)SSCN$ were derived by structure optimizations at fixed dihedral angles between 30° and 330° using the HF and B3LYP method with the basis set of 6-31G* (Figure 1). There is no other minimum except the expected minima for the *gauche* structures with the dihedral angle around 80° (HF/6-31G*) or 90° (B3LYP/6-31G*). And the energy barrier for the S–S rotation is calculated to be 4.42 (HF/6-31G*) and 3.84 (B3LYP/6-31G*) kcal/mol, respectively. This is caused by the S–S lone pair repulsion and steric interactions between $CH_3OC(O)$ and CN moieties. Because of the structural similarity between the title compounds, the situation for $CH_3OC(O)SSeCN$ is probably the same, that is to say, conformers with *gauche* structure around the S–Se bond should be stable. Furthermore, according to the relative orientation of the CH_3O moiety with respect to the C=O bond, which also can be synperiplanar (sp) or antiperiplanar (ap), four possible conformers exist for each of $CH_3OC(O)SSCN$ and $CH_3OC(O)SSeCN$. After structural optimization and vibrational analysis, three conformers of each compound are found to be stable, except the conformers with the C=O bond *anti* to the S–S or S–Se bond and CH_3O *anti* to the C=O bond. The three stable conformers of $CH_3OC(O)SSeCN$ are presented in Figure 2.

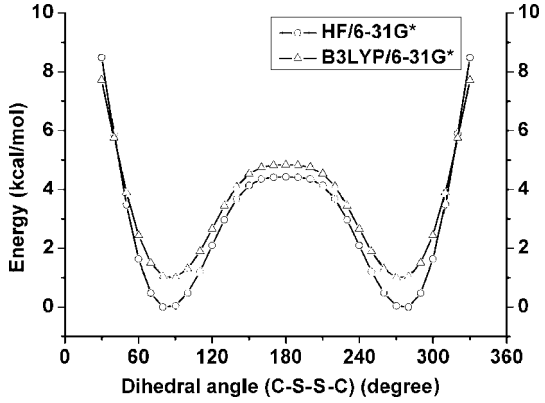

Figure 1. Calculated potential curves for internal rotation around the S–S bond in $CH_3OC(O)SSCN$. The curve of B3LYP/6-31G* is shifted by 1 kcal/mol.

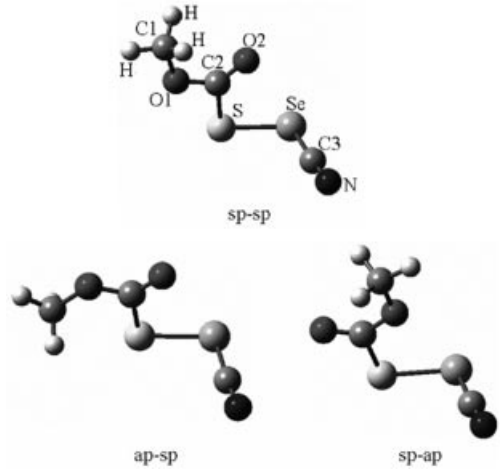

Figure 2. Schematic representation of the three stable conformers of $CH_3OC(O)SSeCN$.

Relative Gibbs free energies (ΔG) calculated at 298 K for all the stable conformers of $CH_3OC(O)SSCN$ and $CH_3OC(O)SSeCN$ are summarized in Table 1. According to these relative Gibbs free energies, the *gauche* (sp-sp) and the *gauche* (sp-ap) conformers are expected to be more stable. All the calculations predict the lowest energy for the *gauche* (sp-sp) conformer. Similar to their parent compound, $CH_3OC(O)SCl$, the structures of $CH_3OC(O)SSCN$ and $CH_3OC(O)SSeCN$ can be rationalized by the aromaticity and the anomeric effect.[23] The stabilization of the *gauche* (sp-sp) conformers are accounted for by the attractive π nonbonded interactions in those conformations. Moreover, the instability of the *anti* conformers in these two molecules can be understood on the basis of the aromaticity. Besides, if one of the central atoms in an A–B–C–D chain, e.g., B, possesses one or more lone pairs, the generalized anomeric effect may have a large influence on the conformational properties.[24] This effect contributes to the preference for the *syn* form for the conformation of –C(O)-S–containing compounds.[25] Our discussion of the geometrical and electronic structures of these two compounds will mainly focus on the theoretically most stable conformers.

Table 1. Calculated relative Gibbs free energies (ΔG, kcal/mol, T = 298 K) for different conformers of $CH_3OC(O)SSCN$ and $CH_3OC(O)SSeCN$.

	HF/6-31+G*	B3PW91/6-31+G*	B3LYP/6-311G*
$CH_3OC(O)SSCN$			
gauche (sp-sp)[a]	0	0	0
gauche (ap-sp)	8.93	6.32	6.93
gauche (sp-ap)	1.09	0.62	0.81
$CH_3OC(O)SSeCN$			
gauche (sp-sp)	0	0	0
gauche (ap-sp)	8.42	5.91	6.94
gauche (sp-ap)	0.60	0.19	0.77

[a] *gauche* refers to the configuration around the S–S or S–Se bond. The first orientation (sp or ap) refers to CH_3O with respect to the C=O bond, and the second orientation (sp or ap) refers to the C=O bond with respect to the S–S or S–Se bond.

The optimized geometrical parameters for the *gauche* (sp-sp) conformer of $CH_3OC(O)SSCN$ and $CH_3OC(O)SSeCN$ at different levels are listed in Table 2.

Table 2. Optimized geometrical parameters for the *gauche* (sp-sp) conformer of $CH_3OC(O)SSCN$ and $CH_3OC(O)SSeCN$.[a]

Parameters	$CH_3OC(O)SSCN$			$CH_3OC(O)SSeCN$		
	B3PW91	B3LYP	MP2	B3PW91	B3LYP	MP2
r_{C1O1}	1.442	1.451	1.445	1.441	1.451	1.445
r_{O1C2}	1.328	1.332	1.337	1.329	1.334	1.339
r_{C2O2}	1.192	1.193	1.201	1.193	1.194	1.202
r_{C2S}	1.818	1.829	1.802	1.819	1.830	1.806
r_{SSe}[b]	2.081	2.102	2.075	2.208	2.231	2.210
r_{SeC3}[b]	1.695	1.703	1.697	1.846	1.856	1.849
r_{C3N}	1.159	1.159	1.181	1.159	1.159	1.182
a_{C1O1C2}	115.7	116.1	114.1	115.6	116.0	113.9
a_{O1C2O2}	127.7	127.7	127.3	127.4	127.4	127.1
a_{O1C2S}	105.7	105.7	105.9	105.7	105.8	105.8
a_{C2SSe}[b]	100.4	100.6	99.3	101.0	101.3	100.0
a_{SSeC3}[b]	101.6	101.8	99.7	99.5	99.7	98.0
$\delta_{C1O1C2O2}$	–0.6	–0.6	–0.8	–0.5	–0.6	–1.3
$\delta_{O1C2SSe}$[b]	177.6	177.6	176.7	178.7	178.8	176.2
$\delta_{C2SSeC3}$[b]	87.6	87.3	80.5	88.6	88.2	80.4

[a] Distances in Å, angles in degrees. All the calculations were performed with the basis set of 6-311++G(d,p). As for the atom numbering of $CH_3OC(O)SSeCN$, see Figure 2. [b] For $CH_3OC(O)SSCN$, Se atoms should be replaced by the corresponding S atoms.

The electronegativity of selenium and sulfur are close to each other. Therefore, the structures of $CH_3OC(O)SSCN$ and $CH_3OC(O)SSeCN$ are similar (Table 2). It is well known that the B3LYP method doesn't do well in modeling relatively weak polar bonds. The MP2 method is believed to be more accurate to obtain the geometry. When optimized with the three methods (Table 2), polarization and diffusion functions were added to assure the calculations were more accurate. The optimized structures with B3LYP and B3PW91 methods, both of which are DFT methods, are nearly identical. Our discussion of the geometry is based on the structures optimized with the MP2 method.

A study on the structural and conformational properties of disulfanes has been reported recently.[7] The conformation of dichalcogens (REE′R′) is mainly determined by the geometry of the EE′ moiety. According to theoretical calculations, the S–S or S–Se bond lengths of $CH_3OC(O)SSCN$ and $CH_3OC(O)SSeCN$ are 2.075 Å and 2.210 Å [MP2/6-311++G(d,p)], respectively. The S–S bond length in $CH_3OC(O)SSCN$ is slightly larger than that of its parent compound, HSSH [2.0610(3) Å].[26] However, there is no experimental work reported about HSSeH. The S–Se bond length in HSSeH was predicted to be 2.269 Å according to ab initio calculations.[19] As determined by X-ray diffraction, the S–Se bond length in NCSSeSCN is 2.214 Å,[21] which is quite close to the predicted value of $CH_3OC(O)SSeCN$.

Besides the E–E′ bond length, another important structural parameter for dichalcogens is the torsional angle $\delta_{REE'R'}$, which greatly influenced the whole structure of the molecules. Gas-phase structures of noncyclic dichalcogens are characterized by the dihedral angle $\delta_{REE'R'}$ close to 90°: for example, HOOH (112°),[27] HSSH [90.76(6)°],[26] and $CH_3SeSeCH_3$ (87.5°).[8] The torsional angle in HSOH was 91.3°, as determined by high-level ab initio calculations [CCSD(T)/cc-pCVQZ].[14] In $CH_3OC(O)SSCN$ and $CH_3OC(O)SSeCN$, the dihedral angles around the S–S or S–Se bond are 80.5° and 80.4° [MP2/6-311++G(d,p)], respectively. The interpretation of the population analysis[28] is consistent with two qualitative arguments about the preference of about 90° of the RSSR′ dihedral angle. A plausible interpretation of the population analysis is related to the resulting barrier formed by the repulsion of 3pπ AO lone pairs. The repulsion is minimized, if these AOs are oriented orthogonal to each other. The second argument[29] is based on a hyperconjugative mechanism, whereby the π-character of the S–S bond is enhanced when, for example in HSSH, the S–H bonds are aligned for maximum transfer of electron density through the 3pπ AOs to the H atom. This feature is consistent with the anomeric effect, that is, the electron donation from the sulfur lone pair into the empty σ* orbitals of the opposite S–H bonds.[24] In other dichalcogens, a similar feature may also exist.

2.2 Photoelectron Spectroscopy

Photoelectron spectroscopy with a HeI resonance source (58.4 nm) is an effective method to investigate electronic structures of unstable compounds and free radicals in combination with ab initio calculations.[30,31] The valence shell structure of molecular vapors can be readily obtained by HeI photoelectron energy analysis, especially for studying similar molecules.[32] The HeI photoelectron spectra of $CH_3OC(O)SSCN$ and $CH_3OC(O)SSeCN$ are shown in Figure 3 and Figure 4, respectively. Before assigning the spec-

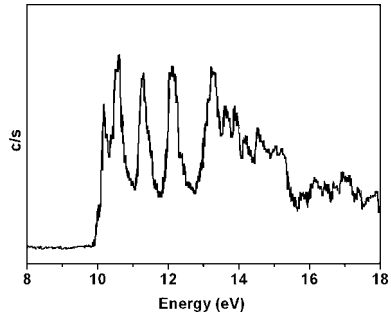

Figure 3. HeI photoelectron spectrum of $CH_3OC(O)SSCN$.

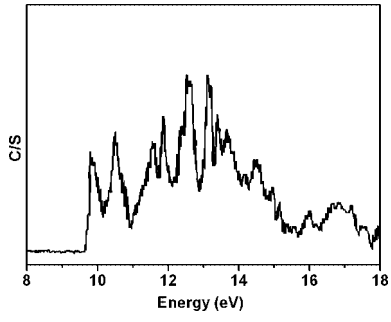

Figure 4. HeI photoelectron spectrum of $CH_3OC(O)SSeCN$.

tra, ROVGF[33] calculations were carried out to obtain the ionization energies for $CH_3OC(O)SSCN$ and $CH_3OC(O)SSeCN$. No noticeable difference can be found between the orbital energies of the two stable conformers of *gauche* (sp-sp) and *gauche* (sp-ap), therefore our discussion is reduced to the analysis of the slightly more stable conformer *gauche* (sp-sp). The experimental vertical ionization potentials, theoretical vertical ionization energies, molecular orbitals, and corresponding characters of outer valence shells for the *gauche* (sp-sp) conformers of $CH_3OC(O)SSCN$ and $CH_3OC(O)SSeCN$ are listed in Table 3. The ROVGF results are in general in agreement with the experimental data. Drawings of nine MOs for $CH_3OC(O)SSCN$ and $CH_3OC(O)SSeCN$ are given in the supporting information.

Table 3. Experimental vertical ionization energies (IP in eV), computed vertical ionization energies [ROVGF/6-311++G(d,p), E_v in eV], and molecular orbital characters for $CH_3OC(O)SSCN$ and $CH_3OC(O)SSeCN$.

Molecule	Exp. IP	Calcd. E_v	MO	Character
$CH_3OC(O)SSCN$				
	10.19	10.27	38	$n_{S(SCN)}$
	10.60	10.64	37	$n_{S(COS)}$
	11.32	11.60	36	$n_{O(C=O)}$
	12.08	12.09	35	σ_{SS}, $\pi_{C\equiv N}$
		12.13	34	$n_{O(CH3O)}$, $n_{O(C=O)}$
	13.26	13.41	33	π_{SCN}
	13.61	13.66	32	σ_{CN}
	13.87	13.93	31	π_{CH3}, $n_{O(CH3O)}$
	14.17	14.19	30	π_{SCN}
$CH_3OC(O)SSeCN$				
	9.84	9.85	47	n_{Se}
	10.56	10.48	46	n_S
	11.54	11.57	45	$n_{O(C=O)}$
	11.84	11.80	44	σ_{SSe}, $\pi_{C\equiv N}$
	12.50	12.05	43	$n_{O(CH3O)}$, $n_{O(C=O)}$
	13.11	13.11	42	$\pi_{C\equiv N}$
	13.41	13.54	41	σ_{CN}
	13.65	13.68	40	π_{CH3}, $n_{O(CH3O)}$
		13.70	39	π_{SeCN}

As pointed out by Baker et al.,[34] for disulfides, peroxides, and diselenides, the first two bands in the photoelectron spectra correspond to the symmetric and antisymmetric linear combinations of the outermost *p*-atomic orbitals. The first two peaks in the photoelectron spectrum of $CH_3OC(O)SSCN$ are centered at 10.19 and 10.60 eV. The main characters for the first two outmost orbitals are $\{38a(n_{S(SCN)})\}^{-1}$ and $\{37a(n_{S(COS)})\}^{-1}$, and the theoretically predicted first two vertical ionization energies are 10.27 and 10.64 eV, respectively, in good agreement with the experimentally observed values. The energy difference ΔE between the first two bands in $CH_3OC(O)SSCN$ (δ_{CSSC} = 80.5°) is 0.41 eV, which is bigger than that of $FC(O)SSCH_3$ [ΔE = 0.3 eV, δ_{CSSC} = 83.5(15)°].[35] This difference is originated by the interaction of the two lone pairs at the adjacent S atoms showing a clear dependence on the dihedral angle. Generally, it is to be expected that as the dihedral angle δ deviates from 90°, the energy difference ΔE will increase, i.e., the 3p orbitals in parallel configuration (δ = 0°, 180°) interact more strongly than in an orthogonal configuration (δ = 90°).[28]

The most peculiar aspects of the photoelectron spectra of the dichalcogens (REE′R′) concern the pattern of the n ionization energies, whose ordering and splitting have been rationalized in terms of the popular concepts of mediated interplay of through-bond and through-space interactions between semilocalized orbitals.[20] In general, the pattern of the splitting is predicted to be $\Delta(OO) > \Delta(SS) \approx \Delta(SeSe)$ for the homonuclear systems and $\Delta(SO) > \Delta(SeS)$ for the heteronuclear; the differences in heteronuclear systems are much larger than those in homonuclear systems.[20] The successive replacement of O by S and Se causes only a progressively minor perturbation of the electronic structure, as is expected from the electronegativity sequence of the chalcogens, O (3.5 on Pauling's scale), S (2.5), and Se (2.4).[20] For sulfenoselenates with the general formula RSSeR′, the splitting of the bands also exists in the photoelectron spectra. The first two peaks in the photoelectron spectrum of $CH_3OC(O)SSeCN$ is centered at 9.84 and 10.56 eV, respectively, which are lower than the corresponding ionization energies of $CH_3OC(O)SSCN$. The energy difference ΔE in $CH_3OC(O)SSeCN$ is 0.72 eV. This difference is larger than that of $CH_3OC(O)SSCN$, but close to its parent compound HSSeH (0.66 eV),[20] as clearly seen from Figure 5.

The third band (11.32 eV) in the photoelectron spectrum of $CH_3OC(O)SSCN$ can be attributed to the n_O electron of the C=O bond, which is similar to the corresponding orbital of the third band (11.54 eV) in that of $CH_3OC(O)SSeCN$. In comparison to the first band of $CH_3OC(O)H$[32] at 10.99 eV $\{13a'(n_{O(C=O)})\}^{-1}$, the inductive effect of the SSCN or SSeCN moiety has raised the ionization energy of the carbonyl oxygen lone pair orbital n_O by 0.33 and 0.55 eV, respectively. The third band in the photoelectron spectrum of $FC(O)SSCH_3$ (11.3 eV),[35] also caused by the ionization of the n_O lone pair, is nearly equal to the corresponding ionization energy of $CH_3OC(O)SSCN$. The ionization from the orbital mainly localized at the σ bond of the SS or SSe moiety and the π orbital on the C≡N moiety causes the energies of 12.08 and 11.84 eV in $CH_3OC(O)SSCN$ and $CH_3OC(O)SSeCN$, respectively. Both are smaller than the ionization energies from $\sigma_{EE'}$ orbitals of their corresponding parent compounds (Figure 5). The differences are caused by the effect of the different substituents on the E–E′ bonds.

The vertical ionization energies from the ionization process of $\{4a''(n_{O(CH3O)}, n_{O(C=O)})\}^{-1}$ in $CH_3OC(O)Cl$ and $CH_3OC(O)CN$ are 12.21 and 12.01 eV, respectively.[32] While in $CH_3OC(O)SSCN$ and $CH_3OC(O)SSeCN$, the corresponding ionization energies are 12.08 and 12.50 eV, respectively. The ionization energies from 13.26 eV to 14.17 eV in $CH_3OC(O)SSCN$ correspond to different orbitals on the SCN moiety. The situation in $CH_3OC(O)SSeCN$ is similar. The electronic structure of the SeCN moiety can be explained in two ways.[17] We can assume a single Se–C bond and a triple C≡N bond, so two bands from the C≡N π bond are expected in the low-energy region of the spectrum. Another interpretation is when the SeCN unit is con-

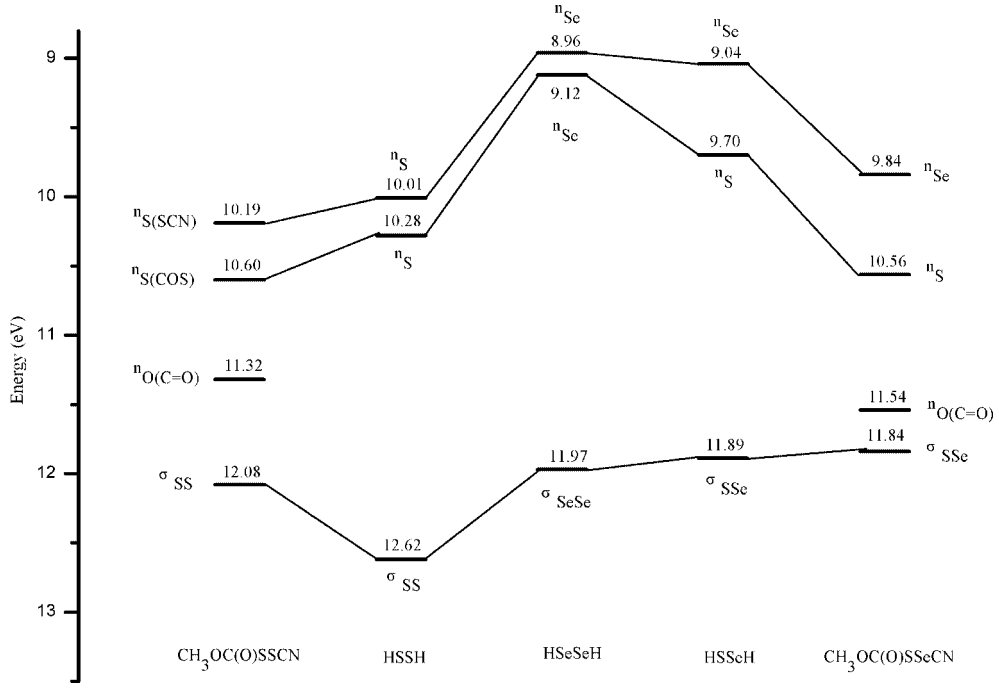

Figure 5. Correlation between selected dichalcogens (REE′R′). The ionization energies of HSSH are taken from ref.,[36] and those of HSeSeH and HSSeH are taken from ref.[20]

sidered as two perpendicular four-electron three-center π systems, which suggests four new bands in the spectrum (the high-energy π_1 and $\pi_{1\perp}$ and the low-energy π_2 and $\pi_{2\perp}$). If the molecular skeleton is linear, the perpendicular MO pairs are degenerate. In the case of the *gauche* $CH_3OC(O)SSeCN$, all four bands are expected theoretically. However, the Se lone pair in the SeCN moiety is part of a π system and the σ_{SSe} orbital is also part of the perpendicular π system. In a word, only two additional bands from the π orbitals of the SeCN moiety are expected in the low-energy region. The assignments for the bands of $CH_3OC(O)SSCN$ and $CH_3OC(O)SSeCN$ agree with this explanation, as summarized in Table 3. The remaining bands in the high-ionization region (>14.5 eV) arising from inner molecular orbitals can not be assigned with certainty.

3. Conclusion

(Methoxycarbonyl)sulfenyl thiocyanate, $CH_3OC(O)SSCN$, and (methoxycarbonyl)sulfenyl selenocyanate, $CH_3OC(O)SSeCN$ are generated and characterized by photoelectron spectroscopy. With the help of quantum chemical calculations, the geometry of the two molecules are investigated and the electronic structure analyzed. Both compounds prefer a *gauche* conformation as predicted by structural optimization and vibrational analysis. The first vertical ionization energies of $CH_3OC(O)SSCN$ and $CH_3OC(O)SSeCN$ are determined to be 10.19 and 9.84 eV, respectively. The HOMOs are mainly localized at the lone pair of the S and Se atom, respectively.

Experimental Section

$CH_3OC(O)SSCN$ and $CH_3OC(O)SSeCN$ were heterogeneously generated at a room temperature of 20 °C by passing $CH_3OC(O)SCl$ vapor over finely powdered AgSCN or AgSeCN, respectively, and the photoelectron spectrum was recorded subsequently after generation. Simultaneously, the product was checked by photoionization mass spectrometry. In the mass spectrum of $CH_3OC(O)SSCN$, there is no signal of the parent ion of the precursor [$CH_3OC(O)SCl^{+}$, m/z = 126], which indicates that $CH_3OC(O)SCl$ reacts with AgSCN completely. However, there are characteristic signals of the product $CH_3OC(O)SSCN$: $CH_3OC(O)SSCN^{+}$ (m/z = 149), $NCSSC(O)^{+}$ (m/z = 118), and $NCSS^{+}$ (m/z = 90). Similarly, in the mass spectrum of $CH_3OC(O)SSeCN$, there are analogously characteristic signals, $CH_3OC(O)SSeCN^{+}$ (m/z = 197), $NCSeSC(O)^{+}$ (m/z = 166), and $NCSeS^{+}$ (m/z = 138), which can confirm the generation of $CH_3OC(O)SSeCN$. The reaction route is illustrated below:

$$CH_3OC(O)SCl\,(g) + AgSCN\,(s) \rightarrow CH_3OC(O)SSCN\,(g) + AgCl\,(s)$$
$$CH_3OC(O)SCl\,(g) + AgSeCN\,(s) \rightarrow CH_3OC(O)SSeCN\,(g) + AgCl\,(s)$$

The precursor $CH_3OC(O)SCl$ was purchased from Alfa Aesar, and used without further purification after confirmation of its identity by obtaining its photoionization mass spectrum. AgSCN was purchased from Alfa Aesar. AgSeCN was prepared according to the previous report[37] by adding a solution of KSeCN to a solution of $AgNO_3$ in stoichiometric amounts. The precipitate formed was collected by filtration, washed with water, and dried in a desiccator under dynamic vacuum. Care should be taken to avoid exposure to light. Before reaction, both silver salts were dried in vacuo (1×10^{-4} Torr) for 2 h.

The photoelectron spectrum was recorded on a double-chamber UPS-II instrument,[16,30] which was specially designed for detecting unstable species. The spectral resolution of the HeI spectrum is

about 30 meV, when measured as the full width at half-maximum (FWHM) of the $3p^{-1}\ ^2P_{2/3}\ Ar^+ \leftarrow Ar\ (^1S_0)$ line. During the experiments, small amounts of Ar gas and CH_3I were added to the sample flow, which were used to calibrate the experimental vertical ionization potentials.

Quantum chemical calculations were performed for the investigated molecules by the Gaussian 03 program package.[38] The structures of all the stable conformers were optimized with ab initio and DFT methods. Higher levels of theory were used to optimize the theoretically most-stable conformers. To interpret the photoelectron spectra, ROVGF[33] calculations with the basis set of 6-311++G(d,p) were performed to obtain the theoretical vertical ionization energies.

Supporting Information (see also the footnote on the first page of this article): Drawings of nine MOs for the *gauche* (sp-sp) conformer of $CH_3OC(O)SSCN$, and drawings of nine MOs for the *gauche* (sp-sp) conformer of $CH_3OC(O)SSeCN$.

Acknowledgments

This project was supported by the Knowledge Innovation Program of the Chinese Academy of Sciences (grant number KZCX2-YW-205) and by the Ministry of Science and Technology of China, Hundred Talents Fund, program 973 (number 2006CB403701), and the National Natural Science Foundation of China (contract numbers 20577052, 20673123, 20473094, 20503035).

[1] C. Bleiholder, D. B. Werz, H. Köppel, R. Gleiter, *J. Am. Chem. Soc.* **2006**, *128*, 2666–2674.
[2] C. Bleiholder, R. Gleiter, D. B. Werz, H. Köppel, *Inorg. Chem.* **2007**, *46*, 2249–2260.
[3] R. Steudel, H. Schmidt, E. Baumeister, H. Oberhammer, T. Koritsanszky, *J. Phys. Chem.* **1995**, *99*, 8987.
[4] H.-G. Mack, C. O. Della Védova, H. Oberhammer, *Angew. Chem. Int. Ed. Engl.* **1991**, *30*, 1145.
[5] A. Hermann, J. Niemeyer, H.-G. Mack, R. Kopitzky, M. Beuleke, H. Willner, D. Christen, M. Schäfer, A. Bauder, H. Oberhammer, *Inorg. Chem.* **2001**, *40*, 1672.
[6] H.-G. Mack, C. O. Della Védova, H. Oberhammer, *J. Phys. Chem.* **1992**, *96*, 9215.
[7] J. G. Breitzer, A. I. Smirnov, L. F. Szczepura, S. R. Wilson, T. B. Rauchfuss, *Inorg. Chem.* **2001**, *40*, 1421–1429.
[8] P. D'Antonio, C. George, A. H. Lowrey, J. Karle, *J. Chem. Phys.* **1971**, *55*, 1071–1075.
[9] J. E. Anderson, L. Henriksen, *J. Chem. Soc. Chem. Commun.* **1985**, 1397–1398.
[10] J. P. Snyder, L. Carlsen, *J. Am. Chem. Soc.* **1977**, *99*, 2931–2942.
[11] S. E. Ulic, C. O. Della Védova, A. Hermann, H.-G. Mack, H. Oberhammer, *Inorg. Chem.* **2002**, *41*, 5699–5705.
[12] S. E. Ulic, A. Kosma, C. Leibold, C. O. Della Védova, H. Willner, H. Oberhammer, *J. Phys. Chem. A* **2005**, *109*, 3739–3744.
[13] S. E. Ulic, A. Kosma, C. O. Della Védova, H. Willner, H. Oberhammer, *J. Phys. Chem. A* **2006**, *110*, 10201–10205.
[14] G. Winnewisser, F. Lewen, S. Thorwirth, M. Behnke, J. Hahn, J. Gauss, E. Herbst, *Chem. Eur. J.* **2003**, *9*, 5501–5510.
[15] R. Gleiter, I. Hyla-Kryspin, H. Schmidt, R. Steudel, *Chem. Ber.* **1993**, *126*, 2363–2365.
[16] X. Zeng, M. Ge, Z. Sun, D. Wang, *J. Phys. Chem. A* **2006**, *110*, 5685–5691.
[17] G. Bajor, T. Veszprémi, E. H. Riague, J.-C. Guillemin, *Chem. Eur. J.* **2004**, *10*, 3649–3656.
[18] R. Laitinen, T. Pakkanen, *J. Mol. Struct. (Theochem)* **1983**, *91*, 337–352.
[19] R. Laitinen, T. Pakkanen, *J. Mol. Struct. (Theochem)* **1985**, *124*, 293–305.
[20] V. Galasso, *J. Electron Spectrosc. Relat. Phenom.* **1984**, *34*, 283–289.
[21] S. Hauge, *Acta Chem. Scand., Ser. A* **1979**, *33*, 313.
[22] P. Sanz, M. Yáñez, O. Mó, *CHEMPHYSCHEM* **2003**, *4*, 830–837.
[23] M. F. Erben, C. O. Della Védova, R. M. Romano, R. Boese, H. Oberhammer, H. Willner, O. Sala, *Inorg. Chem.* **2002**, *41*, 1064–1071.
[24] A. J. Kirby, *The Anomeric Effect and Related Stereoelectronic Effects at Oxygen*, Springer, Berlin, **1983**.
[25] J. R. Larson, N. D. Epiotis, F. Bernardi, *J. Am. Chem. Soc.* **1978**, *100*, 5713–5716.
[26] C. J. Marsden, B. J. Smith, *J. Phys. Chem.* **1988**, *92*, 347–353.
[27] A. M. Halpern, E. D. Glendening, *J. Chem. Phys.* **2007**, *121*, 273.
[28] B. Boyd, *J. Am. Chem. Soc.* **1972**, *94*, 8799.
[29] G. Winnewisser, N. Winnewisser, W. Gordy, *J. Chem. Phys.* **1968**, *49*, 3465.
[30] L. Yao, M. Ge, W. Wang, X. Zeng, Z. Sun, D. Wang, *Inorg. Chem.* **2006**, *45*, 5971–5975.
[31] Z. Sun, S. Zheng, J. Wang, M. Ge, D. Wang, *Chem. Eur. J.* **2001**, *7*, 2995–2999.
[32] X. Zeng, M. Ge, L. Du, Z. Sun, D. Wang, *J. Mol. Struct.* **2006**, *800*, 62–68.
[33] W. von Niessen, J. Schirmer, L. S. Cederbaum, *Comput. Phys. Rep.* **1984**, *1*, 57–125.
[34] A. D. Baker, M. Brisk, M. Gellender, *J. Electron Spectrosc. Relat. Phenom.* **1974**, *3*, 227.
[35] M. F. Erben, C. O. Della Védova, *Inorg. Chem.* **2002**, *41*, 3740–3748.
[36] B. Solouki, H. Bock, *Inorg. Chem.* **1977**, *16*, 665–669.
[37] F. Cataldo, *Polyhedron* **2000**, *19*, 681–688.
[38] M. J. Frisch, G. W. Trucks, H. B. Schlegel, G. E. Scuseria, M. A. Robb, J. R. Cheeseman, J. A. Montgomery Jr, T. Vreven, K. N. Kudin, J. C. Burant, J. M. Millam, S. S. Iyengar, J. Tomasi, V. Barone, B. Mennucci, M. Cossi, G. Scalmani, N. Rega, G. A. Petersson, H. Nakatsuji, M. Hada, M. Ehara, K. Toyota, R. Fukuda, J. Hasegawa, M. Ishida, T. Nakajima, Y. Honda, O. Kitao, H. Nakai, M. Klene, X. Li, J. E. Knox, H. P. Hratchian, J. B. Cross, C. Adamo, J. Jaramillo, R. Gomperts, R. E. Stratmann, O. Yazyev, A. J. Austin, R. Cammi, C. Pomelli, J. W. Ochterski, P. Y. Ayala, K. Morokuma, G. A. Voth, P. Salvador, J. J. Dannenberg, V. G. Zakrzewski, S. Dapprich, A. D. Daniels, M. C. Strain, O. Farkas, D. K. Malick, A. D. Rabuck, K. Raghavachari, J. B. Foresman, J. V. Ortiz, Q. Cui, A. G. Baboul, S. Clifford, J. Cioslowski, B. B. Stefanov, G. Liu, A. Liashenko, P. Piskorz, I. Komaromi, R. L. Martin, D. J. Fox, T. Keith, M. A. Al-Laham, C. Y. Peng, A. Nanayakkara, M. Challacombe, P. M. W. Gill, B. Johnson, W. Chen, M. W. Wong, C. Gonzalez, J. A. Pople, *Gaussian 03 (Revision B.01)*, Gaussian, Inc., Pittsburgh PA, **2003**.

Received: April 26, 2007
Published Online: August 3, 2007

